Observation of Coupled Vortex Lattices in a Mass-Imbalance Bose and Fermi Superfluid Mixture

Xing-Can Yao,[1,2,3,4] Hao-Ze Chen,[1,2,3] Yu-Ping Wu,[1,2,3] Xiang-Pei Liu,[1,2,3] Xiao-Qiong Wang,[1,2,3] Xiao Jiang,[1,2,3] Youjin Deng,[1,2,3] Yu-Ao Chen,[1,2,3] and Jian-Wei Pan[1,2,3,4]

[1]*Shanghai Branch, National Laboratory for Physical Sciences at Microscale and Department of Modern Physics, University of Science and Technology of China, Hefei, Anhui 230026, China*

[2]*CAS Center for Excellence and Synergetic Innovation Center in Quantum Information and Quantum Physics, University of Science and Technology of China, Shanghai 201315, China*

[3]*CAS-Alibaba Quantum Computing Laboratory, Shanghai 201315, China*

[4]*Physikalisches Institut, Ruprecht-Karls-Universität Heidelberg, Im Neuenheimer Feld 226, 69120 Heidelberg, Germany*

(Received 25 July 2016; published 27 September 2016)

Quantized vortices play an essential role in diverse superfluid phenomena. In a Bose-Fermi superfluid mixture, especially of two mass-imbalance species, such macroscopic quantum phenomena are particularly rich due to the interplay between the Bose and Fermi superfluidity. However, generating a Bose-Fermi two-species superfluid, producing coupled vortex lattices within, and further probing interspecies interaction effects remain challenging. Here, we experimentally realize a two-species superfluid with dilute gases of lithium-6 and potassium-41, having a mass ratio of about seven. By rotating the superfluid mixture, we simultaneously produce coupled vortex lattices of the two species and thus present a definitive visual evidence for the double superfluidity. Moreover, we report several unconventional behaviors, due to the Bose-Fermi interaction, on the formation and decay of two-species vortices.

DOI: 10.1103/PhysRevLett.117.145301

Quantized vortices, topological defects of quantized angular momentum, are a direct consequence of macroscopic superfluid wave function [1]. In a superfluid, they crystallize into an Abrikosov lattice pattern [2] that minimizes vortex-vortex interaction. After the celebrated experimental realization of the Bose-Einstein condensate (BEC) [3,4], tremendous theoretical and experimental efforts have been devoted to understanding the behaviors of quantized vortices in BEC and quantum degenerate Fermi gases [5–9], and have yielded a wealth of information and insights into diverse superfluid phenomena.

A superfluid mixture, where both components are superfluid, is a longstanding research topic in quantum physics. A mixture of bosonic ^{4}He and fermionic ^{3}He superfluid is predicted to exhibit either s-wave or topological p-wave Cooper pairs in the ^{3}He component [10], although the superfluid transition of ^{3}He in such a mixture has not been detected down to about 100 μK [11]. In cold atom physics, it is now possible to experimentally produce mixtures of degenerate bosonic and fermionic dilute gases [12–14]. Very recently, a significant progress [15,16] was made in a mixture of two lithium isotopes, ^{6}Li and ^{7}Li, where the evidence of double superfluidity was provided by the occurrence of ^{7}Li BEC and the density-profile difference of the two imbalanced ^{6}Li spins. However, the demonstration of two-species vortices, which not only provide a conclusive evidence but also give fundamental insights into double superfluidity, is still unavailable.

A superfluid mixture of two distinct species, if experimentally realized, can exhibit richer macroscopic quantum phenomena. A large mass imbalance [17,18] may alter the Bose-Fermi interactions, without which a double superfluid is just two independent superfluids. Many fascinating behaviors have been predicted [19], including Bose-Fermi dark-bright solitons [20], polaronic atom-trimer continuity [21], etc. The two-species superfluid of dilute atomic gases can also provide a powerful tool for simulating real materials and beyond, e.g., dense quantum chromodynamics matter [22].

In this Letter, we address the two challenging tasks of generating a two-species superfluid mixture and of producing coupled vortex lattices. By overcoming several technical challenges, we successfully realize a double superfluid of fermionic ^{6}Li and bosonic ^{41}K atoms in an optical dipole trap, which have a mass ratio of about seven. Further, we produce a double-vortex matter in which both superfluid components simultaneously exhibit vortex lattices. Finally, in a series of vortex-number measurements, we observe several unconventional behaviors, due to the interspecies interaction, on the formation and decay of the coupled vortices.

Our first goal is to produce a two-species Bose and Fermi superfluid. We adopt an advanced laser cooling scheme, where a sub-Doppler cooling in gray molasses is implemented for ^{41}K while a near-detuned Doppler cooling is applied for ^{6}Li. After the laser cooling phase, the cold gas mixture is magnetically trapped and transported to a

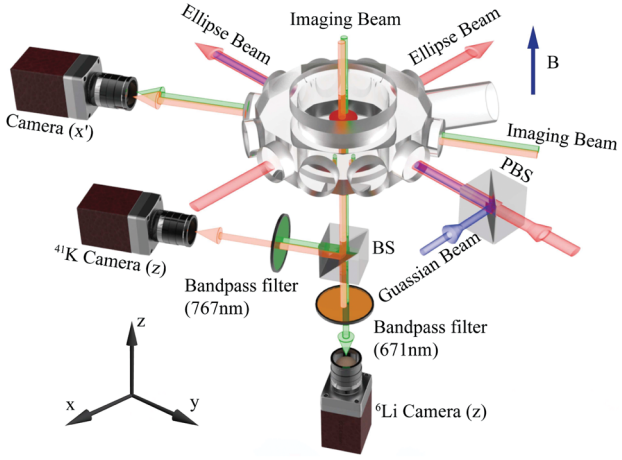

FIG. 1. Sketch of experimental setup. An elliptical beam (light red) is superimposed with a Gaussian beam (blue) by a polarizing beam splitter (PBS), and then crossed with another elliptical beam (light red) at 90°. The dichromatic imaging beams are used for simultaneous absorption imaging of ^{6}Li (green) and ^{41}K (orange) atoms along the z axis. The imaging beams after a beam splitter (BS) are respectively filtered by 671 nm and 767 nm bandpass filters, and then detected by the ^{6}Li and ^{41}K EMCCD cameras. An additional EMCCD camera is used for imaging the two species along the x' axis.

dodecagonal glass cell of good optical access and ultrahigh vacuum environment (see Fig. 1). The first stage evaporative cooling is applied to ^{41}K in an optically plugged magnetic trap by driving $|F=2,m_F=2\rangle$ to $|F=1,m_F=1\rangle$ transition, while ^{6}Li is cooled sympathetically. By optimizing the radio frequency (rf), we achieve a near-degenerate mixture of 5×10^{7} ^{6}Li and 1×10^{7} ^{41}K atoms. Then, the mixture is transferred into a cigar-shaped dipole trap (wavelength 1064 nm, $1/e^2$ radius 35 μm and maximum laser power 10 W), followed by two Landau-Zener sweeps which prepare both species at their lowest hyperfine states. Next, a half-to-half spin mixture of the two lowest hyperfine states of ^{6}Li is prepared by using successive rf sweeps at a magnetic field of 870 G [23]. At this magnetic field, the background scattering length of ^{41}K is $60.5a_0$ (a_0 is the Bohr radius) and that of ^{6}Li-^{41}K is $60.7a_0$ [24,25]. The spin mixture of ^{6}Li is located at the Bardeen-Cooper-Schrieffer (BCS) side of Feshbach resonance with scattering length of $-12580a_0$ [26]. Because of the unitary limited collisional rate between fermionic spins, the forced evaporative cooling of ^{6}Li is rather efficient and ^{41}K is sympathetically cooled.

It is known that the large mass imbalance can induce inhomogeneous spatial overlap or even separation of the two superfluids due to the gravitational sag [27]. After 0.5 s of evaporation in the cigar-shaped trap, the clouds are adiabatically transferred and confined in a disklike trap, where two elliptical laser beams with an aspect ratio of 4:1 are crossed perpendicularly [wavelength 1064 nm, maximum laser power of each beam 1.1 W, $1/e^2$ axial (radial) radius 48 μm (200 μm)]. Subsequent evaporation is achieved by exponentially lowering the laser intensity to 120 mW in 2 s. At the end of evaporation, the trap is held for 1 s to ensure fully thermal equilibrium between both species. The axial trap frequency of ^{6}Li (^{41}K) is 237 Hz (85 Hz), which is strong enough to attain a complete overlap of two superfluids. The horizontal confinement is provided by the combination of magnetic curvature and optical dipole trap, resulting in a radial trap frequency of 40 Hz (20 Hz) for ^{6}Li (^{41}K). A specially designed imaging setup along the z axis is employed to simultaneously probe the two species (see Fig. 1). An imaging resolution of 2.2 μm (2.5 μm) at 671 nm (767 nm) is gained by a high numerical aperture objective, which is very important for observing vortices.

A two-species Bose-Fermi superfluid is finally achieved at 870 G with more than 1.8×10^{5} ^{41}K atoms in a BEC (condensate fraction $\geq 90\%$) and 1.5×10^{6} ^{6}Li atoms at 7% Fermi temperature [15]. The superfluid mixture is very stable, with a $1/e$ lifetime 19 ± 1 s for ^{41}K and 12 ± 0.7 s for ^{6}Li. Figure 2 shows a series of *in situ* images, in which the magnetic field is varied and thus the ultracold spin mixture of ^{6}Li experiences a crossover from a molecular BEC to a BCS superfluid [28]. It can be seen that the radius of the ^{6}Li cloud increases gradually from the BEC to the BCS side, while the ^{41}K cloud size remains unchanged. The geometric centers of the two species are perfectly overlapped in the xy plane, and a full overlap in the gravity direction is also achieved (see Fig. 2). The disklike trap exhibits an approximate rotational symmetry along the z

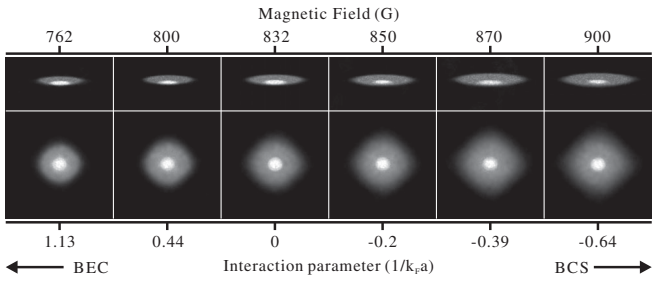

FIG. 2. *In situ* images of two-species Bose-Fermi superfluid of ^{41}K and ^{6}Li. The top and bottom row images, respectively, show the integrated optical density distributions of the two-species superfluid along the x' and z directions, as the magnetic field is varied from the BEC to the BCS side of the ^{6}Li. The ^{6}Li component has an inverse Fermi momentum of $1/k_F\approx0.26$ μm. To take an *in situ* image, we prepare the superfluid mixture at 870 G, ramp the magnetic field to the desired value (from 762 G to 900 G) in 100 ms, and hold the trap for another 100 ms before imaging. Each picture is obtained by carefully superimposing two images that are taken separately in two experimental cycles (top) or simultaneously in a single cycle (bottom). It is seen that the ^{41}K superfluid (bright region) is fully buried in the ^{6}Li superfluid cloud. The viewing scope of top (bottom) images is 416×208 μm^2 (416×416 μm^2).

axis in the center, as shown by the nearly circular shape of the ^{41}K component. The squared shape formed by the edges of the ^{6}Li superfluid reflects an imperfection of the rotational symmetry in a larger scale but might give rise to intriguing vortex structures.

Creating vortex lattices in the two-species superfluid is very complex, arising from several factors like the interspecies interaction and the variation of population ratio. Furthermore, the theoretical optimal stirring parameters for the bosonic and fermionic components are rather distinct due to the difference in size, density, and trap frequency. We explore a wide range of combinations of stirring parameters and successfully find feasible ones. For creation of two-species vortices, the clouds are rotated about their symmetry axis by a blue-detuned laser beam (wavelength 532 nm, $1/e^2$ radius 19 μm) during the last 600 ms of evaporation at 870 G. A two-axis acousto-optic deflector is used to regulate the motion of the stirring beam, where a two-beam pattern with tunable separation is rotated symmetrically with a variable angular frequency [5]. They are then adiabatically turned off, and the trap is held for 2 s. To probe vortices [6], the disklike trap is suddenly switched off and the cloud is expanded in the residual magnetic curvature. During the first 3 ms of expansion the magnetic field is rapidly ramped to 740 G, and the cloud is further expanded for another 17 ms at this field. Absorption imaging for ^{6}Li and ^{41}K atoms are then simultaneously performed.

A series of highly visible coupled vortex lattices are observed (see Fig. 3), as stirring parameters (beam separation, rotating frequency, and stirring-laser power) are varied. Figures 3(a) and 3(d) show a two-species vortex lattice, consisting of an ordered triangular lattice of 20 ^{41}K vortices and 2 symmetric ^{6}Li vortices. An approximately

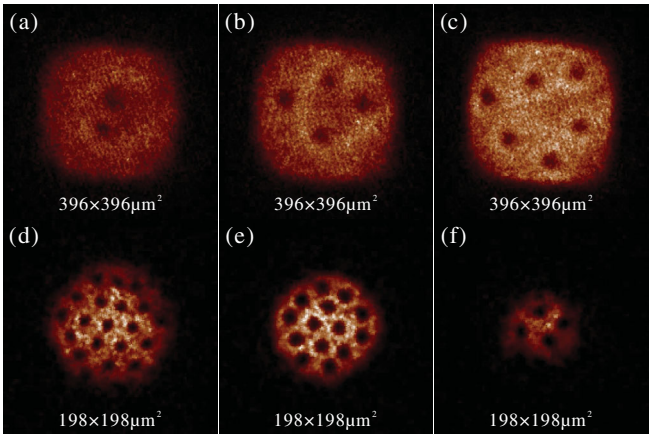

FIG. 3. Coupled vortex lattices in two-species superfluid. The top (bottom) images are for the ^{6}Li (^{41}K) component, and the two images in each column, taken simultaneously in an experimental cycle, are for the same set of stirring parameters. (a),(d) are for separation 28 μm, power 0.75 mW, rotating frequency 26 Hz; (b), (e) are for 52 μm, 0.75 mW, 18 Hz; and (c),(f) are for 76 μm, 1.5 mW, 22 Hz.

regular lattice of 6 ^{6}Li vortices is also obtained [Fig. 3(c)], but only 4 vortices survive in a small ^{41}K condensate [Fig. 3(f)], due to a significantly weakened effective trapping force for ^{41}K. Figures 3(b) and 3(e) contain a diamond of 4 ^{6}Li vortices and a triangular lattice of 14 ^{41}K vortices, respectively. Furthermore, as theoretically predicted [18,29], we observe that the repelling from the ^{41}K superfluid component leads to a density-profile depression in the center of the ^{6}Li component. Such an alternation is also clearly seen in the presence of vortices [Figs. 3(a) and 3(b)]. This implies that the interspecies interaction can play an important role in our system, e.g., on the formation and decay of vortex lattices.

We perform a series of comparison experiments on the formation of vortices, in which the same set of stirring parameters (stirring time 0.6 s, equilibrium time 2 s, laser power 0.75 mW) is respectively applied to the two-species superfluid as well as the single-species superfluid of ^{6}Li or ^{41}K. Furthermore, by adjusting the loading parameters, we also make sure that the temperature and the atom numbers of ^{6}Li and ^{41}K are approximately identical in the single- and the two-species superfluids. A series of measurements are carried out for the average numbers of vortices as a function of rotating frequency. Figure 4 shows four sets of experimental results for different beam separations.

Pronounced effects of the Bose-Fermi interaction are revealed, particularly from the comparison of ^{6}Li vortex numbers (the top row of Fig. 4). Strikingly, in the two-species superfluid the ^{6}Li vortex number is greatly increased and the range of vortex-generation rotating frequency is largely widened. For some ranges of stirring parameters (e.g., 64 μm of beam separation and 46 Hz of rotating frequency), no vortex can be formed in the single-species superfluid of ^{6}Li or ^{41}K, but in the two-species superfluid, the ^{6}Li vortices are unexpectedly created while the ^{41}K vortex is still absent. In addition, we observe that as beam separation is increased, the optimal rotating frequency corresponding to a maximal number of ^{6}Li vortices has a spectacular downshift (from 28 Hz to 22 Hz) in the two-species superfluid while it remains unchanged in the single-species superfluid. These behaviors strongly show that the ^{41}K component acts as an important role in the formation and behavior of ^{6}Li vortices in the two-species superfluid. The coupling effect on generating ^{41}K vortices is less pronounced, but still visible in the shift of the optimal rotating frequency.

We also carry out comparison experiments on the decay of vortices. By adjusting the stirring parameters, the average numbers of ^{6}Li (^{41}K) vortices are initialized to be nearly the same in the single- and two-species superfluids. Figure 5 shows the results of the initial vortex numbers $(2.8 \pm 0.2,\ 19.5 \pm 0.5)$ for ^{6}Li and ^{41}K. Impressively, the ^{6}Li vortices seem more stable in the two-species superfluid than in the single-species superfluid, with a $1/e$

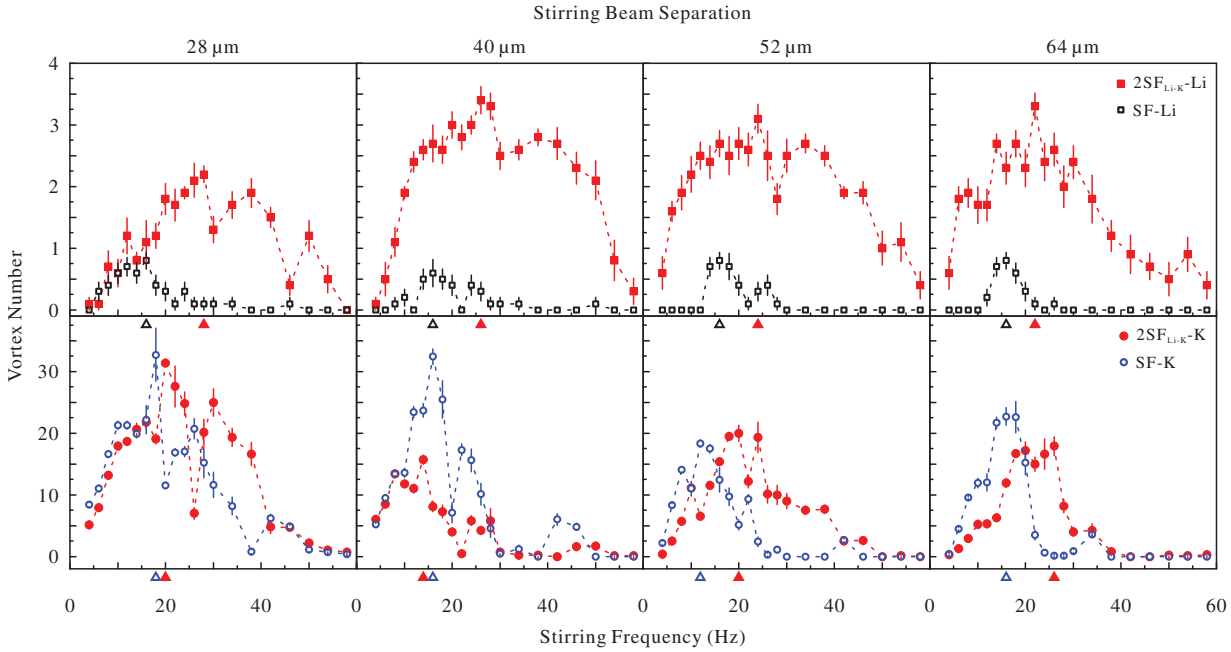

FIG. 4. Comparison of vortex numbers in single- and two-species superfluids. For a given set of stirring parameters, three comparison experiments are respectively performed for the superfluid mixture and the single-species superfluid of ^{6}Li or ^{41}K. Vortex numbers are counted and statistically averaged over 10 measurements with standard error margin being calculated. 2SF$_{Li-K}$-Li (2SF$_{Li-K}$-K) represents ^{6}Li (^{41}K) component of two-species superfluid; SF-Li (SF-K) represents single species ^{6}Li (^{41}K) superfluid. For each column of plots, the beam separation is fixed, while the rotating frequency is varied. Optimal frequencies for creating a maximal number of vortices are indicated by the filled (open) triangles on the horizontal axis with the same color of the data points. The interspecies interaction effects can be clearly seen from the dramatic difference of the ^{6}Li vortex numbers (top row), over a wide range of rotating frequency.

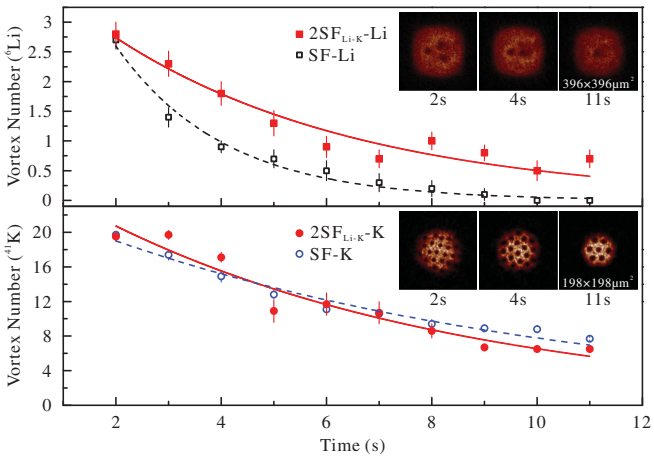

FIG. 5. Decay of vortices in single- and two-species superfluids. Three comparison experiments are carried out with the initial ^{6}Li (^{41}K) vortex numbers being set approximately identical (see text). 2SF$_{Li-K}$-Li (2SF$_{Li-K}$-K) represents ^{6}Li (^{41}K) component of two-species superfluid; SF-Li (SF-K) represents single species ^{6}Li (^{41}K) superfluid. Each data point has a standard error bar and is gained by averaging over 10 measurements. The curves are obtained by fitting the experimental data to an exponential decay. The insets show typical images of vortices in the two-species superfluid, suggesting the survival of both ^{6}Li and ^{41}K vortices after 11 s.

lifetime $\tau_2 = 4.7 \pm 0.5$ s twice long as $\tau_1 = 2.1 \pm 0.2$ s. In contrast, the ^{41}K vortex lifetimes are $\tau_2 = 6.9 \pm 0.5$ s for the superfluid mixture and $\tau_1 = 9.1 \pm 0.6$ s for the single-species superfluid.

In the rotating superfluid mixture, it is plausible that the Bose-Fermi interaction would lead to energy and/or angular-momentum transfer between the bosonic and fermionic components. Over a wide range of stirring parameters, the number of ^{41}K vortices is roughly 7 times larger than that of ^{6}Li vortices, equal to the mass ratio. Further, the life-time ratio of single-species vortices $\tau_{1,\mathrm{Li}}/\tau_{1,K} \sim 0.2$ is significantly enhanced to $\tau_{2,\mathrm{Li}}/\tau_{2,K} \sim 0.7$ for the two-species superfluid. According to the Onsager-Feynman relation [30,31], which states that the vortex-number density is proportional to the product of atom mass and superfluid angular frequency, we conjecture that the angular frequencies of the Bose and Fermi superfluid components are roughly the same. We stress that theoretical insights are desired to reveal the underlying mechanisms of the observed unconventional behaviors on the formation and decay of coupled vortices. With deeper understanding, one might expect to predict a variety of novel macroscopic quantum phenomena, arising from the interplay of Bose and Fermi superfluidity.

In summary, we have employed a combination of state-of-the-art techniques, including advanced laser cooling

scheme, specially designed disklike optical trap, etc., and produced a two-species Bose-Fermi superfluid, containing more than 1.8×10^5 ^{41}K atoms and 1.5×10^6 ^{6}Li atoms. Our work represents important progress in experimentally realizing a superfluid mixture of two distinct species, a longstanding goal in cold-atom physics. Vortex lattices are successfully generated and directly visualized in the two-species superfluids, providing a conclusive evidence for the peculiar state of Bose-Fermi double superfluidity. The large mass imbalance of ^{41}K and ^{6}Li can lead to pronounced effects of interspecies interaction, as clearly revealed in the formation and decay of two-species vortices that request theoretical explanations. With a wide range of tunable parameters like the population ratio of two species, magnetic field controlling the BEC-BCS crossover and stirring parameters, many static and dynamic properties of such Bose-Fermi superfluid mixtures can be explored, particularly those due to interspecies coupling, vortex-vortex interaction, and their interplay.

We are indebted to valuable discussions with A. Leggett, K. Chen, and H. Zhai. This work has been supported by the NSFC of China, the CAS, and the National Fundamental Research Program (under Grant No. 2013CB922001). X.-C. Y. acknowledges support from the Alexander von Humboldt Foundation.

[1] E. M. Lifshits and L. P. Pitaevskii, *Statistical Physics*, Vol. 5 (Pergamon, Oxford, 1980).
[2] A. A. Abrikosov, Zh. Eksp. Teor. Fiz. **32**, 1442 (1957). [Sov. Phys. JETP **5**, 1174 (1957)].
[3] M. H. Anderson, J. R. Ensher, M. R. Matthews, C. E. Wieman, and E. A. Cornell, Science **269**, 198 (1995).
[4] K. B. Davis, M. O. Mewes, M. R. Andrews, N. J. van Druten, D. S. Durfee, D. M. Kurn, and W. Ketterle, Phys. Rev. Lett. **75**, 3969 (1995).
[5] K. W. Madison, F. Chevy, W. Wohlleben, and J. Dalibard, Phys. Rev. Lett. **84**, 806 (2000).
[6] M. W. Zwierlein, J. R. Abo-Shaeer, A. Schirotzek, C. H. Schunck, and W. Ketterle, Nature (London) **435**, 1047 (2005).
[7] M. W. Zwierlein, A. Schirotzek, C. H. Schunck, and W. Ketterle, Science **311**, 492 (2006).
[8] S. Giorgini, L. P. Pitaevskii, and S. Stringari, Rev. Mod. Phys. **80**, 1215 (2008).
[9] A. L. Fetter, Rev. Mod. Phys. **81**, 647 (2009).
[10] J. Rysti, J. Tuoriniemi, and A. Salmela, Phys. Rev. B **85**, 134529 (2012).
[11] J. Tuoriniemi, J. Martikainen, E. Pentti, A. Sebedash, S. Boldarev, and G. Pickett, J. Low Temp. Phys. **129**, 531 (2002).
[12] A. G. Truscott, K. E. Strecker, W. I. McAlexander, G. B. Partridge, and R. G. Hulet, Science **291**, 2570 (2001).
[13] F. Schreck, L. Khaykovich, K. L. Corwin, G. Ferrari, T. Bourdel, J. Cubizolles, and C. Salomon, Phys. Rev. Lett. **87**, 080403 (2001).
[14] G. Roati, F. Riboli, G. Modugno, and M. Inguscio, Phys. Rev. Lett. **89**, 150403 (2002).
[15] I. Ferrier-Barbut, M. Delehaye, S. Laurent, A. T. Grier, M. Pierce, B. S. Rem, F. Chevy, and C. Salomon, Science **345**, 1035 (2014).
[16] M. Delehaye, S. Laurent, I. Ferrier-Barbut, S. Jin, F. Chevy, and C. Salomon, Phys. Rev. Lett. **115**, 265303 (2015).
[17] R. Zhang, W. Zhang, H. Zhai, and P. Zhang, Phys. Rev. A **90**, 063614 (2014).
[18] T. Ozawa, A. Recati, M. Delehaye, F. Chevy, and S. Stringari, Phys. Rev. A **90**, 043608 (2014).
[19] A. B. Kuklov and B. V. Svistunov, Phys. Rev. Lett. **90**, 100401 (2003).
[20] M. Tylutki, A. Recati, F. Dalfovo, and S. Stringari, New J. Phys. **18**, 053014 (2016).
[21] Y. Nishida, Phys. Rev. Lett. **114**, 115302 (2015).
[22] K. Maeda, G. Baym, and T. Hatsuda, Phys. Rev. Lett. **103**, 085301 (2009).
[23] K. E. Strecker, G. B. Partridge, and R. G. Hulet, Phys. Rev. Lett. **91**, 080406 (2003).
[24] S. Falke, H. Knöckel, J. Friebe, M. Riedmann, E. Tiemann, and C. Lisdat, Phys. Rev. A **78**, 012503 (2008).
[25] E. Tiemann, H. Knöckel, P. Kowalczyk, W. Jastrzebski, A. Pashov, H. Salami, and A. J. Ross, Phys. Rev. A **79**, 042716 (2009).
[26] G. Zürn, T. Lompe, A. N. Wenz, S. Jochim, P. S. Julienne, and J. M. Hutson, Phys. Rev. Lett. **110**, 135301 (2013).
[27] R. Pires, J. Ulmanis, S. Häfner, M. Repp, A. Arias, E. D. Kuhnle, and M. Weidemüller, Phys. Rev. Lett. **112**, 250404 (2014).
[28] Q. Chen, J. Stajic, S. Tan, and K. Levin, Phys. Rep. **412**, 1 (2005).
[29] K. Mølmer, Phys. Rev. Lett. **80**, 1804 (1998).
[30] L. Onsager, Nuovo Cimento **6**, 279 (1949).
[31] R. P. Feynman, in *Progress in Low Temperature Physics*, Vol. I (North-Holland, Amsterdam, 1955).